Grain orientation mapping in gradient nanostructured metals produced by surface plastic deformation

Huang, X.; Zhu, M.; Feng, Z. Q. ; He, Q. Y.; Wu, G. L. ; Schmidt, S.

Published in:
Advanced Metallic Materials by Microstructural Design

Publication date:
2017

Document Version
Publisher's PDF, also known as Version of record

Grain orientation mapping in gradient nanostructured metals produced by surface plastic deformation

X Huang[1], M Zhu[2], Z Q Feng[2,3], Q Y He[2], C S Hong[1], G L Wu[2], S Schmidt[4]

[1] Section for Materials Science and Advanced Characterization, Department of Wind Energy, Risø Campus, Technical University of Denmark, DK-4000, Roskilde, Denmark
[2] College of Materials Science and Engineering, Chongqing University, Chongqing 400045, China
[3] Electron Microscopy Center of Chongqing University, Chongqing University, Chongqing 400045, China
[4] Department of Physics, Technical University of Denmark, DK-2800 Kgs. Lyngby, Denmark

Email: xihu@dtu.dk

Abstract. Surface gradient nanostructured metals characterized by grain size and grain orientation variations from the surface to the interior can be produced by surface plastic deformation. Grain orientation mapping allows a quantitative characterization of both the microstructural and textural gradients that determine the properties and performance of such surface deformed metals. Two-dimensional (2D) orientation mapping techniques in a scanning electron microscope and a transmission electron microscope are typically used to generate grain orientation maps in surface gradient nanostructured metals. In this paper, examples of such grain orientation maps are given to show the advantages and limitations of 2D grain orientation mapping. The challenges associated with the indexing of superimposed electron diffraction patterns are discussed in particular, leading to the conclusion that solving this problem can ultimately only be achieved by 3D orientation mapping.

1. Introduction

A variety of techniques involving surface plastic deformation have been developed for generating gradient nanostructures at a metal surface, including surface mechanical attrition treatment (SMAT) [1-3], modified shot-peening [4-6], surface mechanical grinding treatment (SMGT) [7,8], frictional sliding deformation [9–11], and high pressure surface rolling (HPSR) [12]. Two important characteristics associated with the resulting surface gradient nanostructures are the microstructural gradient and the textural gradient [4,8,10], which result from the strain gradient and strain rate gradient generated by the applied surface plastic deformation. The details of the structural and textural gradients depend therefore on the processing technique (deformation mode), the processing conditions (the magnitude of strain and strain rate, generation of heat during processing, etc.), and materials parameters (initial grain size, texture and composition, etc.). A precise characterization of the microstructural and textural gradients is of great importance to understand the improvement of properties and performance of treated metallic components with such gradients.

Two-dimensional (2D) grain orientation mapping techniques, including scanning electron microscope-based electron backscatter diffraction (SEM-based EBSD) [4,8,11,12], and transmission electron microscope-based precession electron diffraction (TEM-based PED) [13-15] have been used [16-18] to characterize the gradient structure and texture. In this paper we first present examples of applying these techniques to generate grain orientation maps in selected samples, to reveal some common features in the microstructural and textural gradients in surface plastic-deformed samples. We then discuss the advantages and limitations associated with these techniques, pointing out the need for three-dimensional (3D) orientation mapping to allow a precise and complete characterization of the microstructure and texture in gradient nanostructures.

2. Grain size scales in gradient nanostructured metals

The typical gradient microstructure feature produced by surface plastic deformation is illustrated in figure 1, which shows an SEM electron channeling contrast (ECC) image of the entire deformed layer in a sample of pure Cu processed by the HPSR technique [12], from the surface (dashed line) to the coarse grain undeformed matrix (2 mm away from the surface). The boundary spacing (grain size) measured from high magnification ECC observations [12] and EBSD orientation maps (see figure 2) reveals a finest boundary spacing of about 50 nm at the topmost surface layer. Even finer surface grain sizes have been obtained in Cu treated by other surface plastic deformation techniques. Hughes and Hansen reported [9] a boundary spacing of 5 nm at the surface of a Cu-0.5%Fe alloy produced by applying a large sliding load in liquid nitrogen. Fang et al. reported a 20 nm grain size in the topmost layer in pure Cu processed by SMGT [7]. The finest grain size is arguably the most important parameter to consider when choosing a grain orientation mapping technique. In the following, two examples of grain orientation mapping by 2D SEM-based EBSD and TEM-based PED techniques are given to show how microstructural and textural information can be obtained in surface gradient nanostructured metals.

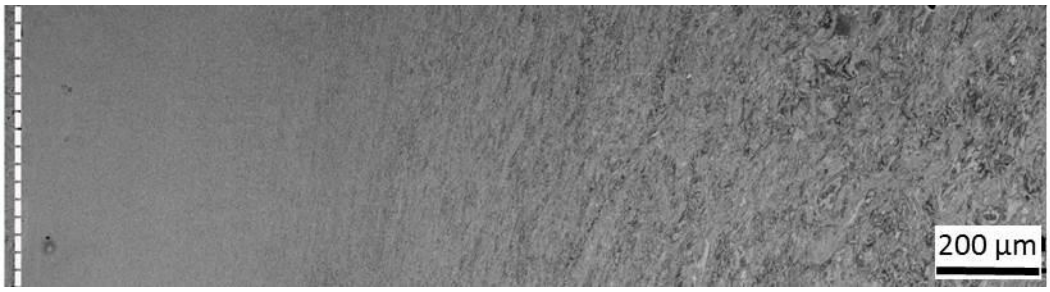

Figure 1. A low magnification ECC image from the tangential section of pure Cu processed by high pressure surface rolling [12]. The dashed line marks the surface.

3. Grain orientation mapping by SEM-based EBSD

Grain orientation maps taken along the depth direction in the surface-deformed Cu shown in figure 1 were generated from EBSD measurements in a field-emission gun SEM [12]. Example maps are shown in figure 2. The black dots in these maps indicate unindexed points. A gradient structure from the topmost surface to the coarse grained bulk is clearly observed in figure 2(a-d). The black layer on the left side of figure 2(a) corresponds to the microstructure in the top ~10 µm in figure 1, where the fine grains and a high density of defects within the grains do not allow EBSD to resolve the details of the microstructure. At depths of 10-600 µm, a higher indexing fraction rate of about 73-75% was achieved. The orientation maps (figure 2(a) and (b)) reveal a lamellar structure parallel to the sample surface with a gradual increase of the boundary spacing from 110 nm at a depth of ~20 µm to about 580 nm at a depth of 600 µm. The indexing fraction further increases to 84% in the depth range of 600-1200 µm where a transition region composed of the lamellar structure and a slightly refined grain

layer is observed (figure 2(c)). At depths greater than 1200 μm, the indexing fraction is about 95% (figure 2(d)). The right part of figure 2(d) shows that the grains are slightly deformed but otherwise are not very different from the annealed microstructure at depths larger than 2000 μm.

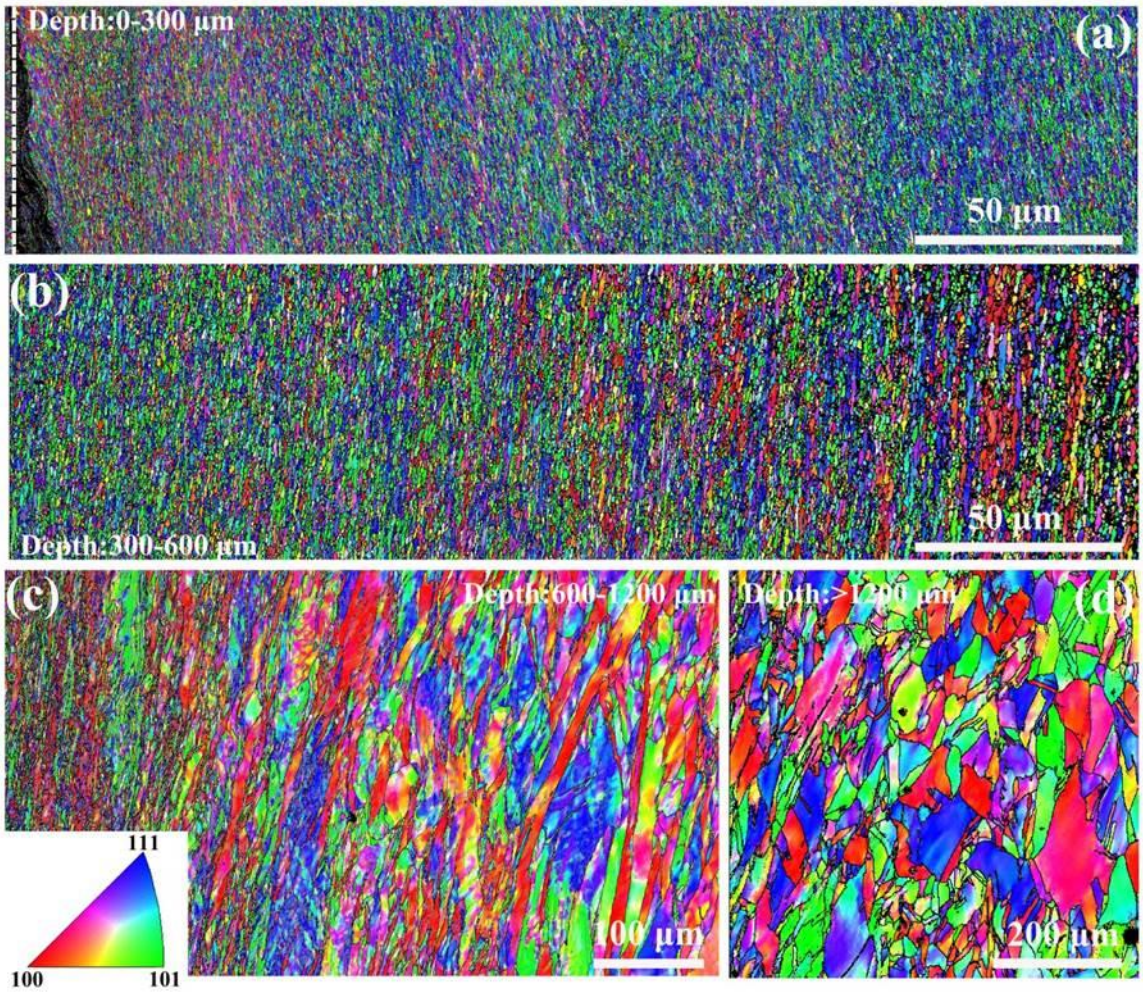

Figure 2. EBSD maps at various depths from the surface in Cu treated by high pressure surface rolling [12] (same sample as shown in figure 1). (a) 0-300 μm, (b) 300-600 μm, (c) 600-1200 μm, and (d) >1200. The white dashed line in (a) indicates the surface. The unindexed points are shown in black, which are related to grain boundaries and second phase particles.

Figure 3 shows {111} pole figures at different depths illustrating the evolution of texture in the surface-deformed Cu sample. Here ND refers to the normal direction of the surface-deformed plate and RD refers to the rolling direction (the tangential direction of the rotating rollers used in the surface-deformation process) [12], which is parallel to the vertical direction in the EBSD map in figure 2. It is seen that in the surface region (0-75 μm) a weak shear texture with dominant {001}<110> and {111}<110> components is formed. It is interesting to see that the shear texture strengthens in the volume 75-300 μm from the surface. At larger depths (300-450 μm) the dominant texture components are close to Brass and Copper. With further increase of depth from the surface the texture is less developed. The development of well-defined shear texture components in the surface region suggests that the HPSR processing results in strong shear deformation at the surface, similar to that during sliding [9] and SMGT [7].

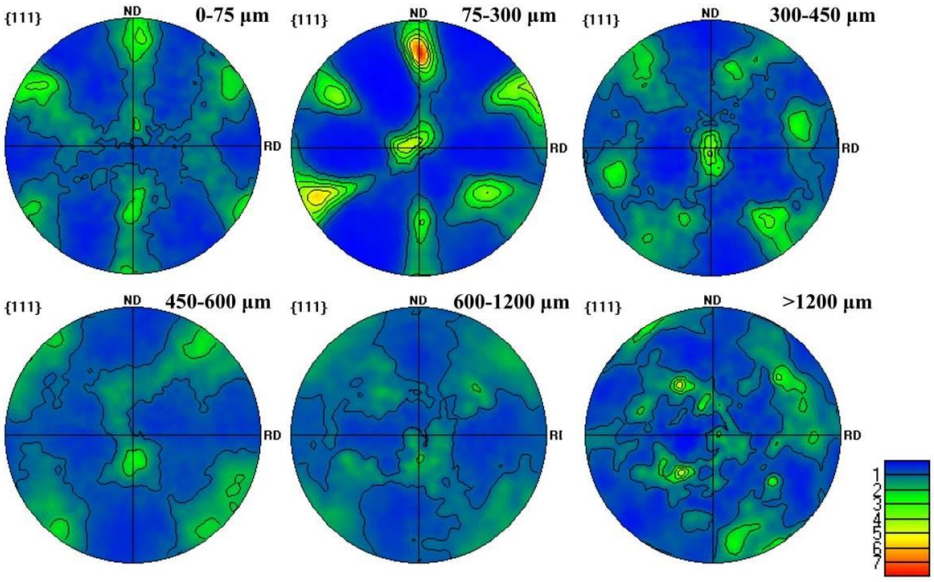

Figure 3. {111} pole figures generated from the EBSD data shown in figure 2. Note that the original EBSD data set was divided into subsets along the depth for plotting the pole figures.

4. Grain orientation mapping by TEM-based PED

An automated crystal orientation mapping technique based on precession electron diffraction in the TEM has been developed and proven to be a useful quantitative method for grain size and texture analysis with a spatial resolution down to a few nanometers [13-15]. This technique has been applied to map grain orientations in the surface gradient nanostructures of several metals and alloys [16-18] after different surface plastic deformation treatments. Figure 4 shows an example of orientation maps obtained in a commercial Ni-based superalloy plate processed by flat surface mechanical grinding [16]. The plate surface normal direction is defined as ND and the grinding direction is defined as SD [16]. Figure 4a shows SD and ND inverse pole figure orientation maps covering only the topmost 1.3µm-thick layer [16]. A clear gradient structure is seen, composed of a 350nm-thick layer of mixed equiaxed and lamellar nanograins, and a 650nm-thick lamellar nanograin layer. Deformation twins (indicated by arrows) as fine as 8 nm were recognized by indexing the related PED patterns, such as those shown in figure 4(c) and (d). Based on the PED orientation mapping, the crystallographic texture of the surface deformed layer was identified as a mixture of a strong shear texture component {001}<110> and a minor Copper component {112}<111>. The formation of shear texture components is a result of the shear deformation introduced by the surface grinding process.

5. Discussion

Gradient nanostructures produced by surface plastic deformation have two characteristic features, namely that the finest grain sizes formed at the topmost surface can reach a few nanometers and that the grains contain a high density of internal lattice defects (dislocations) [7-9]. These characteristics generate challenges in analyzing the orientation of individual grains when using different orientation mapping techniques. SEM-based EBSD orientation mapping is normally applicable to coarser grains (> 20nm) both because of the spatial resolution limit and the sensitivity of EBSD pattern quality to the presence of lattice defects within grains [13,14]. Therefore the conventional EBSD technique has been

mainly used to map the structure and obtain texture information for regions below the deformed surface where the boundary spacing is larger than about 50 nm and the dislocation density is relatively low [8,10-12]. Such limitations associated with the conventional EBSD technique are well-known and have been well documented in the literature [13,14,19,20], and will thus not be discussed further.

A crucial challenge for the TEM-PED method is to determine the orientations in the topmost layer of gradient nanostructures, where the electron signal comes from overlapping grains, as will be illustrated and discussed further in the following.

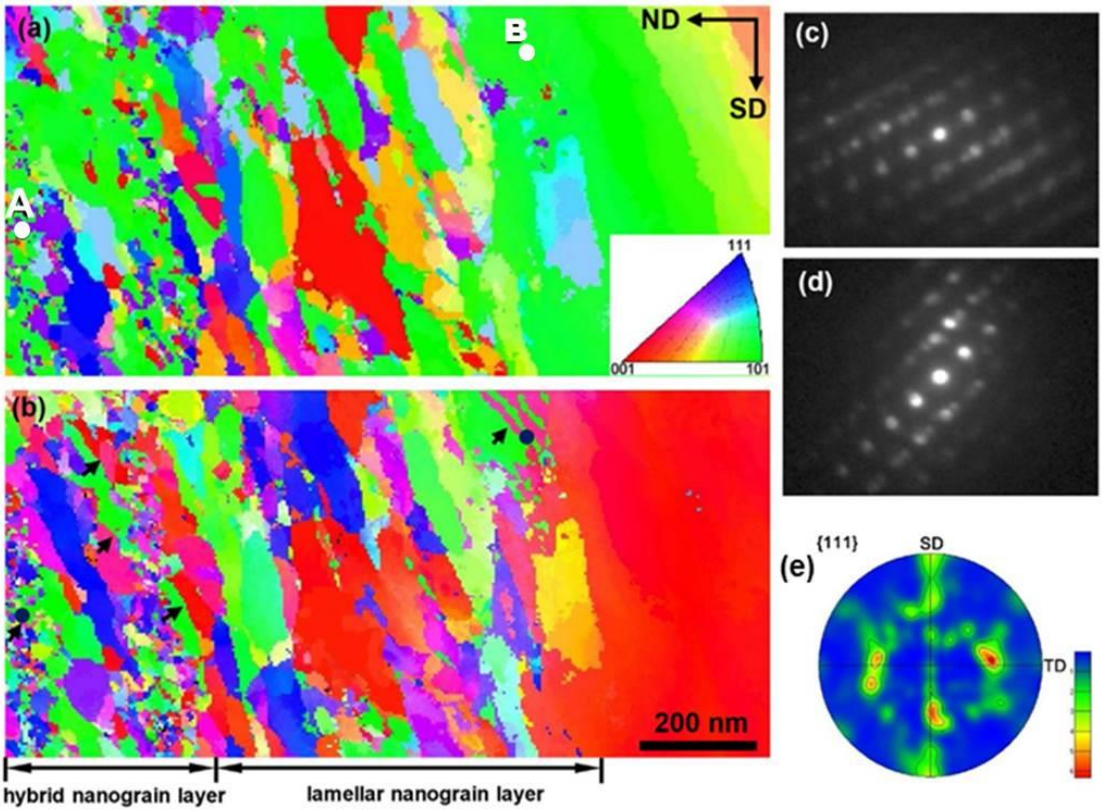

Figure 4. TEM-based PED orientation maps obtained in the topmost surface layer of a Ni-based alloy plate sample processed by a surface mechanical grinding treatment [17]. (a,b) SD and ND inverse pole figure orientation maps. (c,d) PED patterns obtained from locations A and B as shown in (a) containing fine deformation twins. (e) {1 1 1} pole figure obtained from the entire region.

Figure 5 shows examples of possible situations where grains overlapping through the sample thickness may generate difficulties in correctly indexing grain orientations. The situation on the far left shows the ideal case where there is only a single grain through the sample thickness and therefore results in a single diffraction pattern that can be easily indexed. When two or more grains are overlapping along the electron beam direction (the remaining cases shown in figure 5), more complicated diffraction patterns will be formed, with one or more sets of dominant diffraction patterns present depending on the orientation or volume dominance. In the orientation-dominated case one grain has a low index zone axis close to the beam direction and thus forms a diffraction pattern with a high intensity. In the case of a large grain with such an orientation dominance, the diffraction pattern may be dominated by one spot pattern even though the electron beam has passed through more than one grain. A more general and complicated case is where several grains with similar dominance of orientation and volume are overlapping, and the corresponding diffraction pattern is a superposition of

patterns with similar intensities from the overlapping grains. This will cause confusion in the PED template-matching procedure. Figure 6 shows such an example, which was obtained from the location indicated by a black dot in figure 6(a) near the surface of the deformed sample. A superimposed PED pattern (figure 6(b)) composed of four candidate diffraction patterns from <011>, <214>, <215> and <114> zone axes (see figure 6(c)) is recorded. In particular the diffraction patterns for the <214>, <215> and <114> zone axes show similar reflection intensities and correlation index reliability values based on the template matching between the experimental and simulated diffraction patterns. However only the <215> zone axis was selected during the indexing procedure as the most reliable orientation and this orientation was assigned to the location (grain). This unique selection of orientation may cause an incorrect orientation map as no spatial information regarding the through-thickness location of the indexed grains is available, and as such grains seen as adjacent on the projected 2D map may not in fact be neighboring grains in the sample volume.

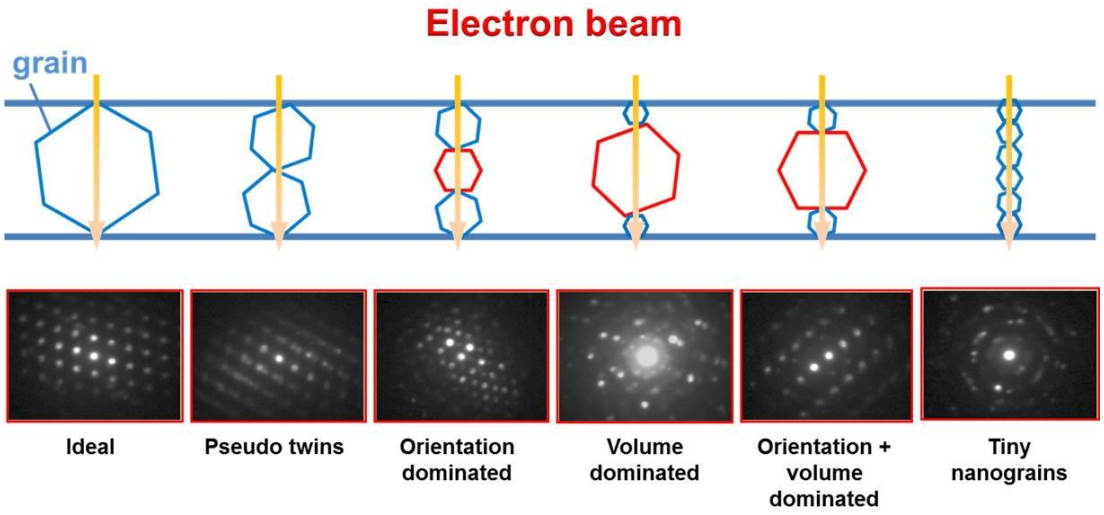

Figure 5. Examples of possible situations of grain overlapping that may cause difficulties in indexing grain orientation and generating reliable grain orientation maps.

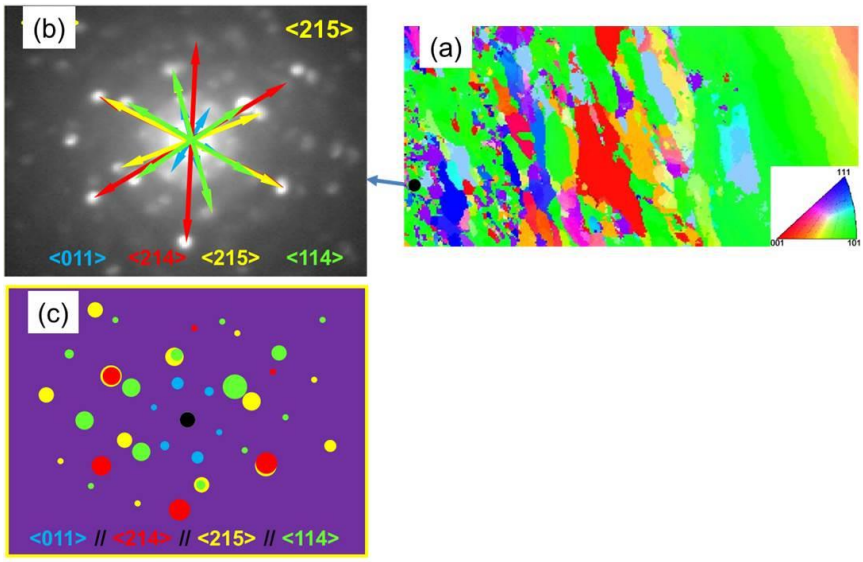

Figure 6. An example showing superimposition of several diffraction patterns with similar reflection intensities.

In a recent study [21] Bobler and Kübel discussed in detail the challenges in quantitative crystallographic characterization by TEM-based spot diffraction method including PED. In their study they collected data for a tilt series over a tilt angle range of 10° for a nanocrystalline Pd thin film to see how the overlapping grains were revealed at different tilts. They showed that many overlapping grains appeared and disappeared depending on the tilt angle and the evaluation parameters chosen for the cross-correlation between the experimental and simulated (template) diffraction patterns. The results revealed that some orientations were more dominant than others during the template-matching procedure between experimental and simulated diffraction patterns, and that a high reliability was not a sufficient criterion to exclude overlapping grains [21].

The challenge in indexing superimposed diffraction patterns from overlapping grains is an inherent problem in the study of nanostructured materials for any TEM-based technique, including the 2D conical dark field scanning technique [22,23], as well as for the SEM-based transmission Kikuchi diffraction (TKD) method [19,20], which has a better spatial resolution than the conventional EBSD method. To distinguish the diffraction signal from overlapping nanograins, 3D orientation mapping techniques are required. 3D orientation mapping based on acquiring diffraction patterns for every pixel, at every tilt, is possible [24-26] if individual diffraction signals from superimposed diffraction patterns can be separated, for example using the principal component analysis method [27]. However, such a direct diffraction tomography technique for 3D grain orientation mapping is not yet available. Instead, a 3D orientation mapping technique has been developed based on conical dark field scanning over a large region of reciprocal space and using a series of sample tilts [28]. This technique enables a precise and complete identification of the size, orientation, location and neighborhood relationship of grains in the sample volume. The current issues with this technique are the data acquisition speed, possible distortion of the 3D grain orientation map caused by the missing wedge effect, and the robustness of 3D reconstruction algorithm. Further development of the technique for 3D orientation mapping in the TEM (3D-OMiTEM) is in progress to address these issues.

6. Concluding remarks

Surface plastic deformation can serve as an approach to produce surface gradient nanostructures in metals and alloys with characteristic microstructural and textural gradients. SEM-based EBSD and TEM-based PED techniques have been applied to obtain grain orientation maps, providing useful information on the microstructural and textural gradients. However, limitations and challenges still remain for both types of techniques. The SEM-based EBSD technique, despite significant technological development in recent years, is still limited by the pattern source volume to a resolution in the order of 20-50 nm, which is insufficient to measure accurately orientations of nanograins at the topmost layer of gradient nanostructured metals. The TEM-based PED method has been proven to be able to measure the orientation of grains as fine as a few nanometers. However, a challenge to correctly distinguish and solve superimposed diffraction patterns from overlapping grains aligned along the beam direction remains. A similar problem exists also for the TEM-based 2D conical dark field scanning technique and the SEM-based TKD method. Tomographic methods such as the 3D orientation mapping in the TEM (3D-OMiTEM) technique provide an ultimate solution to fully identify both the orientation and exact location of overlapping grains in a given sample volume. However, rapid data collection procedures, together with robust orientation determination and 3D reconstruction software to allow routine use of this technique are still under development.

Acknowledgement

Part of the present work is supported by the National Natural Science Foundation of China (51541101, 51671039) and the State Key Research and Development Program (2016YFB0700403).

References

[1] Lu K and Lu J 1999 *J Mater Sci Technol* **15** 193–7

[2] Tong W P, Tao N R, Wang Z B, Lu J and Lu K 2003 *Science*. **299** 686–8

[3] Wu X, Jiang P, Chen L, Yuan F and Zhu Y T 2014 *Proc. Natl. Acad. Sci. U.S A.* **111** 7197–201
[4] Zhang X, Hansen N, Gao Y and Huang X 2012 *Acta Mater.* **60** 5933-43
[5] Liu G, Lu J and Lu K 2000 *Mater. Sci. Eng. A* **286** 91–5
[6] Wang X, Li Y S, Zhang Q, Zhao Y H and Zhu Y T 2016 *J. Mater. Sci. Technol.***15** 193-7
[7] Fang T H, Li W L, Tao N R and Lu K 2011 *Science* **331** 1587–90
[8] Liu X C, Zhang H W and Lu K 2013 *Science* **342** 337
[9] Hughes D and Hansen N 2001 *Phys. Rev. Lett.* **87** 135503
[10] Hong C, Huang X and Hansen N, 2015 *IOP Conf. Series: Materials Science and Engineering* **89** 12026
[11] Deng S Q, Godfrey A, Liu W and Hansen N 2016 *Scr. Mater.* **117** 41
[12] He Q Y, Zhu M, Mei Q S, Hong C S, Wu G L and Huang X 2017 *Proceedings of the 38th Risø International Symposium on Materials Science, IOP Conference Series: Materials Science and Engineering*
[13] Rauch E F, Portillo J, Nicolopoulos S, Bultreys D, Rouvimov S and Moeck P 2010 *Z. Für Krist.* **225** 103–9
[14] Zaefferer S 2011 *Cryst. Res. Technol.* **46** 607–28
[15] NanoMEGAS, www.nanomegas.com
[16] Feng Z Q, Chen Y X, Wu G L and Yang Y Q 2015 Proceedings of the 36th Risø International Symposium on Materials Science, IOP Conference Series: Materials Science and Engineering vol 89(IOP Publishing)p 12023
[17] Chen, Y X, Yang Y Q, Feng Z Q, Huang B, Luo X and Zhao G M, 2017 *Phil. Mag.* **97** 28-42
[18] Chen, Y X, Yang Y Q, Feng Z Q, Zhao G M, Huang B, Luo X, Zhang Y S and Zhang W, 2017 *Mater. Charact. 123* 189-97
[19] Keller R R and Geiss R H 2012 *J. Microsc.* **245** 245–51
[20] Trimby P W 2012 *Ultramicroscopy* **120** 16–24
[21] Kobler A and Kübel C 2017 *Ultramicroscopy* **173** 84–94
[22] Dingley D J 2006 *Microchim. Acta* **155** 19–29
[23] Wu G and Zaefferer S 2009 *Ultramicroscopy* **109** 1317–25
[24] Eggeman A S, Krakow R and Midgley P A 2015 *Nat. Commun.* **6** 7267
[25] Eggeman A S, Krakow R and Midgley P A 2015 Acta Crystallogr. A **70** 12020
[26] Thomas J M, Leary R K, Eggeman A S and Midgley P A 2015 *Chem. Phys. Lett.* **631**–**632** 103–13
[27] Sinkler W and Marks L D, 2009, *Z. Für Krist*. **225** 1-20
[28] Liu H H, Schmidt S, Poulsen H F, Godfrey A, Liu Z Q, Sharon J A and Huang X 2011 *Science* **332** 833–4